

**On the  $\pi^+\pi^-$  and  $D_s^+\pi^\pm$  mass spectra in the  $D_{s1}(2536) \rightarrow D_s^+\pi^+\pi^-$  decays**

Jorgivan Morais Dias <sup>1,\*</sup> Yi-Yao Li <sup>2,3,4,5,†</sup> and Eulogio Oset <sup>5,6,‡</sup>

<sup>1</sup>*Departamento de Física, Universidade Federal do Piauí, 64049-550 Teresina, Piauí, Brasil*

<sup>2</sup>*State Key Laboratory of Nuclear Physics and Technology, Institute of Quantum Matter, South China Normal University, Guangzhou 510006, China*

<sup>3</sup>*Key Laboratory of Atomic and Subatomic Structure and Quantum Control (MOE), Guangdong-Hong Kong Joint Laboratory of Quantum Matter, Guangzhou 510006, China*

<sup>4</sup>*Guangdong Basic Research Center of Excellence for Structure and Fundamental Interactions of Matter, Guangdong Provincial Key Laboratory of Nuclear Science, Guangzhou 510006, China*

<sup>5</sup>*Departamento de Física Teórica and IFIC, Centro Mixto Universidad de Valencia-CSIC Institutos de Investigación de Paterna, 46071 Valencia, Spain*

<sup>6</sup>*Department of Physics, Guangxi Normal University, Guilin 541004, China*

## Abstract

We have carried out an evaluation of the  $\pi^+\pi^-$  and  $D_s^+\pi^+$  mass distributions in the  $D_{s1}(2536)$  decay to  $D_s^+\pi^+\pi^-$ , from the perspective that the  $D_{s1}(2536)$  is a molecular state, mostly made from  $DK^*$  in  $I = 0$ . We are able to obtain, not only the mass distributions, but the branching ratio of this decay. The shape of the mass distributions differ appreciably from those of the analogous reaction  $D_{s1}(2460) \rightarrow D_s^+\pi^+\pi^-$ , which has been measured by the LHCb collaboration and analyzed theoretically from the perspective that the  $D_{s1}(2460)$  is a molecular state of  $D^*K$ , showing a good agreement with the data. In spite of the analogy with the  $D_{s1}(2460)$  decay, the dynamical differences in the decay mechanism are important, since now the  $f_0(500)$  resonance is not generated, while it was the dominant mechanism in the  $D_{s1}(2460) \rightarrow D_s^+\pi^+\pi^-$  decay. Nonetheless, we find striking differences in the mass distributions compared with phase space as a consequence of the decay mechanism. The branching ratio obtained is an order of magnitude bigger than the one of the  $D_{s1}(2460) \rightarrow D_s^+\pi^+\pi^-$  reaction, mostly due to the larger available phase space. Hence, its measurement could be done, and it would shed light on the nature of the  $D_{s1}(2536)$  resonance and indirectly on that of the  $D_{s1}(2460)$ .

## I. INTRODUCTION

Over the past two decades, numerous new hadronic states have been observed, many of which do not fit into the conventional quark configurations predicted by the quark model, that is,  $q\bar{q}$  for mesons, and  $qqq$  for baryons [1–4]. While these discoveries challenge our understanding of the strong interaction, they also provide a natural laboratory to explore the complexity and richness of Quantum Chromodynamics (QCD) in the low-energy regime [5, 6].

Most of the experimental observations, as well as the corresponding theoretical studies, have focused on hadrons in the heavy-quark sector, involving either charm or bottom. In contrast, systems containing both charm and strangeness remain relatively unexplored, despite the existence of some experimental data available for quite some time—as is the case of the  $D_{s1}(2536)$  resonance, with quantum numbers  $J^P = 1^+$ .

---

\* [jorgivan.dias@ufpi.edu.br](mailto:jorgivan.dias@ufpi.edu.br)

† [liyiyao@m.scnu.edu.cn](mailto:liyiyao@m.scnu.edu.cn)

‡ [eulogio.oset@ific.uv.es](mailto:eulogio.oset@ific.uv.es)

In particular, the  $D_{s1}(2536)$  state was first observed in 1989 by the ARGUS Collaboration in  $e^+e^-$  collisions at the DESY storage ring [7]. Its mass was measured as  $(2535.9 \pm 0.6 \pm 2.0)$  MeV, with a narrow width of less than 4.6 MeV. Since then, this state has been confirmed by other collaborations, including CLEO [8], BaBar [9, 10], Belle [11], and more recently LHCb [12].

There have been some attempts to describe not only the structure of the  $D_{s1}(2536)$  meson, but also to establish a broader understanding of the spectroscopy of mesons containing both charm and strangeness — namely, the  $D_s$  mesons [13–17]. Specifically, the  $D_{s1}(2536)$  has quantum numbers  $J^P = 1^+$  and is therefore an axial-vector resonance [10, 18, 19]. In principle, this structure is interpreted as a quark configuration of the type  $c\bar{s}$ . However, mass predictions from potential models based on HQET [20] are in disagreement with experimental data. This discrepancy also extends to other  $D_{s1}$  structures, such as the  $D_{s1}(2460)$  [21]. In particular, the predicted values from quark models [16] lie well above the  $D^*K$  and  $DK^*$  thresholds, corresponding to the  $D_{s1}(2460)$  and the  $D_{s1}(2536)$ , respectively. On the other hand, hadronic structures near meson-meson thresholds can be well described as molecular-type states using the molecular model [5]. In Refs. [22–26], both the  $D_{s1}(2460)$  and the  $D_{s1}(2536)$  are interpreted as dynamically generated states arising from the interactions between pseudoscalar and vector mesons, with the  $D^*K$  and  $DK^*$  channels playing a dominant role in the formation of the  $D_{s1}(2460)$  and  $D_{s1}(2536)$ , respectively.

The molecular interpretation finds strong support in the successful description of the hadronic properties of several resonances, both in the heavy-quark sector and in the light sector [27–44]. As a result, this framework has been extensively explored, with many studies proposing reactions in which such properties can be measured, putting the molecular picture to the test [45]. This may shed light on the current debate surrounding the interpretation of these states as more complex structures, often referred to by the term exotic.

From this perspective, the reaction  $D_{s1}(2460) \rightarrow D_s^+\pi^+\pi^-$  was studied in Ref. [46], assuming a molecular  $D^*K$  interpretation for the  $D_{s1}(2460)$  meson, and also in Ref. [47] including contributions from the  $D_s\eta$  channel, and using a different formalism. In this approach, the decay proceeds via triangle loop diagrams. In particular, the configuration of the intermediate states in the loop allows for the manifestation of resonances such as the  $f_0(500)$  and even the  $f_0(980)$  in the unitarized amplitudes associated with the interactions between pseudoscalar mesons [30, 48, 49]. A key point in favor of this mechanism, as applied

to the reaction discussed in Ref. [46, 47], is its good agreement with the corresponding experimental data reported by the LHCb Collaboration for the decay  $D_{s1}(2460) \rightarrow D_s^+ \pi^+ \pi^-$  [50]. Indeed, such agreement supports the molecular interpretation of the  $D_{s1}(2460)$  meson.

Following this line of thought, we assume in the present work that the  $D_{s1}(2536)$  structure is also interpreted as a molecular state, dynamically generated by the  $DK^*$  interaction, as suggested in Ref. [23]. In order to test its molecular nature, we compute the invariant mass spectra of the  $D_s^+ \pi^\pm$  and  $\pi^+ \pi^-$  pairs, which are among the final products of the decay  $D_{s1}(2536) \rightarrow D_s^+ \pi^+ \pi^-$ . In particular, we adopt the mechanism in which the  $D_{s1}(2536)$  meson decays into  $D_s^+ \pi^+ \pi^-$  via a triangular loop, with  $D$ ,  $K^*$ , and  $K$  mesons as intermediate states, in analogy to the successful mechanism employed in Ref. [46, 47]. Through the interactions between the  $D$  and  $K$  mesons, the final states  $D_s^+ \pi^+$  and  $\pi^+ \pi^-$  are produced, enabling the calculation of the relevant spectra. This mechanism has no free parameters, since the cutoff in the loop integral is fixed by the  $DK^*$  interaction, as discussed in Ref. [23]. As a result, our parameter-free predictions yield absolute results that allow for a direct comparison with experiment, once future measurements of this reaction become available. In Ref. [47] the absolute rate of  $D_{s1}(2460) \rightarrow D_s^+ \pi^+ \pi^-$  was also evaluated and found compatible with experiment within errors. This gives us confidence in the predictions for the rate of the  $D_{s1}(2536) \rightarrow D_s^+ \pi^+ \pi^-$  decay.

This work is organized as follows: in Section II, we present in detail the formalism employed to evaluate the decay  $D_{s1}(2536) \rightarrow D_s^+ \pi^+ \pi^-$ . In particular, we describe the mechanism through which the reaction proceeds, and introduce the relevant triangle diagrams that contribute to this reaction. In the same section, we explicitly evaluate the triangle amplitudes associated with each diagram. Next, in Section III, we present the numerical results for the invariant mass spectra of the  $\pi^+ \pi^-$  and  $D_s^+ \pi^\pm$  pairs, discussing in detail the physical implications of the corresponding lineshapes. Moreover, we compute the decay width of the  $D_{s1}(2536)$  into the  $D_s^+ \pi^+ \pi^-$  channel without the use of free parameters. Finally, in Section IV, we summarize our main results and present our conclusions.

## II. FORMALISM

In our model, the decay  $D_{s1}(2536) \rightarrow D_s^+ \pi^+ \pi^-$  occurs via triangle loops, illustrated in Fig. 1. In particular, we assume that the meson  $D_{s1}(2536)$  is a molecular state  $DK^*$ , whose

coupling to this channel is given in Ref. [51]. In Fig. 1, as a further step in the process, the meson  $K^*$  decays into a pair of pseudoscalar mesons, namely:  $K$  and  $\pi$ . The meson  $K$ , thus produced, interacts with the meson  $D$  originally generated at the vertex  $D_{s1}DK^*$ , and the  $DK$  pair undergoes a transition to the final  $D_s\pi$  meson state, whose distribution interests us. The  $D_{s1}(2536)$  has  $I = 0$ . With isospin phase convention

$$K = \begin{Bmatrix} K^{*+} \\ K^{*0} \end{Bmatrix}, \quad D = \begin{Bmatrix} D^+ \\ -D^0 \end{Bmatrix}, \quad (1)$$

the  $K^*D$  wave function of the  $D_{s1}(2536)$  is  $|K^*D, I = 0\rangle = -\frac{1}{\sqrt{2}}(K^{*+}D^0 + K^{*0}D^+)$ . The coupling of  $D_{s1}(2536)$  to the  $|K^*D, I = 0\rangle$  state is  $g_{D_{s1}(2536),K^*D,I=0} = 20234 \text{ MeV}$  [51], and then  $g_{D_{s1}(2536),K^{*+}D^0} = g_{D_{s1}(2536),K^{*0}D^+} = -\frac{1}{\sqrt{2}}g_{D_{s1}(2536),K^*D,I=0}$ . The vertex of  $D_{s1}(2536) \rightarrow K^{*+}D^0$  corresponding to Fig. 1(a) is given by

$$V_{D_{s1}(2536) \rightarrow K^{*+}D^0} = g_{D_{s1}(2536),K^{*+}D^0} \vec{\epsilon}_A \vec{\epsilon}_{K^*}, \quad (2)$$

with  $\vec{\epsilon}_A$  the polarization vector for the axial meson state  $D_{s1}(2536)$ .

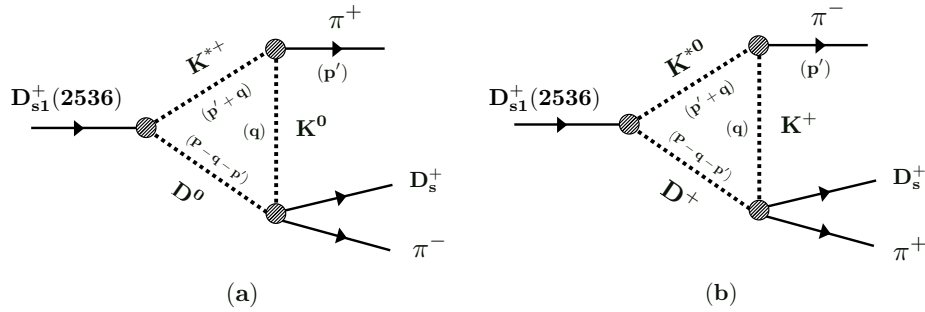


FIG. 1.  $D_{s1}$  decay mechanism: (a) Decay through the  $D^0 K^{*+}$  component, while in (b), the  $D_{s1}$  meson decays through the  $D^+ K^{*0}$  component.

To calculate the amplitudes in Fig. 1, we first need to compute the upper vertices of the  $VPP$  type ( $V$  for vector and  $P$  for pseudoscalar mesons). This can be easily obtained with the help of the effective Lagrangians of the Local Hidden Gauge approach [52–55].

Specifically, for the  $VPP$  vertices, we have

$$\mathcal{L} = -i g \langle [P, \partial_\mu P] V^\mu \rangle, \quad (3)$$

where  $g = M_V/2f$ , with  $M_V = 800$  MeV, an average vector mesons mass, while  $f$  is the pion decay constant, equal to 93 MeV, and the symbol  $\langle \dots \rangle$  denotes the trace of the SU(3) matrices. Additionally,  $P$  and  $V^\mu$  correspond to the matrices  $q_i \bar{q}_j$  in terms of quarks, given in terms of the physical pseudoscalar and vector mesons, respectively, by

$$P = \begin{pmatrix} \frac{\pi^0}{\sqrt{2}} + \frac{\eta}{\sqrt{3}} & \pi^+ & K^+ & \bar{D}^0 \\ \pi^- & -\frac{\pi^0}{\sqrt{2}} + \frac{\eta}{\sqrt{3}} & K^0 & D^- \\ K^- & \bar{K}^0 & -\frac{\eta}{\sqrt{3}} & D_s^- \\ D^0 & D^+ & D_s^+ & \eta_c \end{pmatrix}, \quad (4)$$

$$V = \begin{pmatrix} \frac{\rho^0}{\sqrt{2}} + \frac{\omega}{\sqrt{2}} & \rho^+ & K^{*+} & \bar{D}^{*0} \\ \rho^{*-} & -\frac{\rho^0}{\sqrt{2}} + \frac{\omega}{\sqrt{2}} & K^{*0} & D^{*-} \\ K^{*-} & \bar{K}^{*0} & \phi & D_s^{*-} \\ D^{*0} & D^{*+} & D_s^{*+} & J/\psi \end{pmatrix}, \quad (5)$$

where we take into account the standard  $\eta - \eta'$  mixing, as discussed in Ref. [56]. Thus, considering the momenta defined in Fig. 1, we obtain the following expression for the relevant  $VPP$  vertices

$$V_{VPP} = g \varepsilon_\mu (q - p')^\mu, \quad (6)$$

where  $\varepsilon_\mu$  is the polarization vector of the meson  $K^*$ .

Next, we need to calculate the transitions  $D^0 K^0 \rightarrow D_s^+ \pi^-$ ,  $D^+ K^+ \rightarrow D_s^+ \pi^+$ , which appear at the lower vertices of the diagrams in Fig. 1. These  $PP \rightarrow PP$  transitions (with  $P$  standing for pseudoscalar meson) can be easily computed using an extension of the Local Hidden Gauge approach [52–55]. They were calculated in Ref. [47]. Specifically, for the  $D^0 K^0 \rightarrow D_s^+ \pi^-$  we have

$$V_{K^0 D^0 \rightarrow D_s^+ \pi^-} = \frac{1}{4f^2} \frac{1}{2} \left[ 3s - (m_{K^0}^2 + m_{\pi^-}^2 + m_{D^0}^2 + m_{D_s^+}^2) - \frac{1}{s} (m_{D^0}^2 - m_{K^0}^2) (m_{D_s^+}^2 - m_{\pi^-}^2) \right], \quad (7)$$

where  $s \equiv M_{\text{inv}}^2(D_s^+ \pi^-)$ .

Due to isospin symmetry, the transition potentials for the processes  $D^0 K^0 \rightarrow D_s^+ \pi^-$  and  $D^+ K^+ \rightarrow D_s^+ \pi^+$  are identical in both magnitude and sign. This follows from the fact that both initial two-meson states couple to a total isospin  $I = 1$ , differing only in their third component  $I_3$ . Furthermore, by carefully considering the conventional phase assignments of the isospin multiplets—particularly the  $(-\pi^+, \pi^0, \pi^-)$  basis for pions and the  $D, K$  isospin phase conventions given above—the relative phases between the physical states ensure that no additional sign difference arises between these transitions. Consequently, the interaction potential derived for the  $D^0 K^0 \rightarrow D_s^+ \pi^-$  channel in Eq. (7) can be directly applied to the  $D^+ K^+ \rightarrow D_s^+ \pi^+$  channel.

Once the relevant vertices for calculating the diagrams in Fig. 1(a)-(b) have been obtained, we can write the corresponding amplitudes for the triangle loops under consideration. Next, we will discuss in detail the loop in Fig. 1(a), while the calculation for the diagram in Fig. 1(b) follows analogously. With the upper vertices  $K^{*+} \pi^+ K^0$  and  $K^{*0} \pi^- K^+$  at hand, and considering Eq. (7) for the transition  $D^0 K^0 \rightarrow D_s^+ \pi^-$ , the diagram in Fig. 1(a) can be written as

$$\begin{aligned}
-i t_{\text{loop}}^{(a)} &= \int \frac{d^4 q}{(2\pi)^4} (-i) g_{D_{s1}(2536), K^{*+} D^0} \varepsilon_{Ai} \varepsilon_{K^*i} \frac{i}{(p' + q)^2 - m_{K^*}^2 + i\varepsilon} (-i) g \varepsilon_{K^* \alpha} (q - p')^\alpha \\
&\times \frac{i}{q^2 - m_K^2 + i\varepsilon} \frac{i}{(P - p' - q)^2 - m_D^2 + i\varepsilon} (-i) V_{D^0 K^0 \rightarrow D_s^+ \pi^-}, \quad (8)
\end{aligned}$$

with  $P$  standing for the momentum of the  $D_{s1}(2536)$ .

Assuming we are dealing with small three-momenta compared to the masses of the particles involved, it implies that only the spatial components of the polarization vector of  $K^*$  meson are non-vanishing, that is <sup>1</sup>

$$\varepsilon_{K^*}^0 = \frac{|\vec{p}' + \vec{q}|}{m_{K^*}} \simeq 0, \quad (9)$$

and the completeness relation for the corresponding polarization vectors, which reads

$$\sum_{\text{pol}} \varepsilon_{K^* \mu} \varepsilon_{K^* \alpha} = -g_{\mu\alpha} + \frac{(p' + q)_\mu (p' + q)_\alpha}{m_{K^*}^2}, \quad (10)$$

can now be written as

$$\sum_{\text{pol}} \varepsilon_{K^* \mu} \varepsilon_{K^* \alpha} \simeq \sum_{\text{pol}} \varepsilon_{K^* i} \varepsilon_{K^* j} \simeq \delta_{ij}. \quad (11)$$

---

<sup>1</sup> Actually, the correction from keeping the  $\varepsilon^0$  component goes as  $\left(\frac{\vec{p} + \vec{q}}{m_{K^*}}\right)^2$ , multiplied by a coefficient that renders the correction even smaller (see appendix A of [57])

Therefore, using Eq. (11), the triangle amplitude reduces to

$$\begin{aligned}
- it_{\text{loop}}^{(a)} &= \int \frac{d^4 q}{(2\pi)^4} (-i) g_{D_{s1}(2536), K^{*+} D^0} \varepsilon_{A_i} \varepsilon_{K_i^*} \frac{i}{(p' + q)^2 - m_{K^*}^2 + i\varepsilon} (-i) g \varepsilon_{K^* j} \\
&\times (p' - q)_j \frac{i}{q^2 - m_K^2 + i\varepsilon} \frac{i}{(P - p' - q)^2 - m_D^2 + i\varepsilon} (-i) V_{D^0 K^0 \rightarrow D_s^+ \pi^-}. \quad (12)
\end{aligned}$$

The  $K^{*+}$  and  $D^0$  mesons in Fig. 1(a) are close to being on-shell such that we can consider only the positive energy part in their propagators, that is

$$\begin{aligned}
\frac{1}{(p' + q)^2 - m_{K^*}^2 + i\varepsilon} &\simeq \frac{1}{2\omega_{K^*}(\vec{p}' + \vec{q})} \frac{1}{p'^0 + q^0 - \omega_{K^*}(\vec{p}' + \vec{q}) + i\varepsilon}, \\
\frac{1}{(P - q - p')^2 - m_D^2 + i\varepsilon} &\simeq \frac{1}{2\omega_D(\vec{p}' + \vec{q})} \frac{1}{P^0 - p'^0 - q^0 - \omega_D(\vec{p}' + \vec{q}) + i\varepsilon}, \quad (13)
\end{aligned}$$

where  $\omega_{K^*}(\vec{p}' + \vec{q}) = \sqrt{(\vec{p}' + \vec{q})^2 + m_{K^*}^2}$ ,  $\omega_D(\vec{p}' + \vec{q}) = \sqrt{(\vec{p}' + \vec{q})^2 + m_D^2}$ ,  $\omega_K(\vec{q}) = \sqrt{\vec{q}^2 + m_K^2}$  (for later use), and  $\vec{P} = 0$  in the  $D_{s1}$  rest frame. On the other hand, for the  $K$  meson, we keep both positive and negative energy parts since it is a lighter meson and can be more off shell. Hence, Eq. (12) can be rewritten as

$$\begin{aligned}
t_{\text{loop}}^{(a)} &= i g g_{D_{s1}(2536), K^{*+} D^0} V_{D^0 K^0 \rightarrow D_s^+ \pi^-} \varepsilon_{A_i} \int \frac{d^4 q}{(2\pi)^4} (p' - q)_i \frac{1}{2\omega_{K^*}} \frac{1}{2\omega_K} \frac{1}{2\omega_D} \\
&\times \frac{1}{p'^0 + q^0 - \omega_{K^*}(\vec{p}' + \vec{q}) + i\varepsilon} \frac{1}{P^0 - p'^0 - q^0 - \omega_D(\vec{p}' + \vec{q}) + i\varepsilon} \\
&\times \left( \frac{1}{q^0 - \omega_K(\vec{q}) + i\varepsilon} - \frac{1}{q^0 + \omega_K(\vec{q}) - i\varepsilon} \right). \quad (14)
\end{aligned}$$

Now, we can perform an analytical integration over the  $q^0$  variable, using Cauchy's residue theorem, so that Eq. (14) now assumes the following form

$$\begin{aligned}
t_{\text{loop}}^{(a)} &= g g_{D_{s1}(2536), K^{*+} D^0} V_{D^0 K^0 \rightarrow \pi^- D_s^+} \vec{\varepsilon}_{A_i} \int \frac{d^3 q}{(2\pi)^3} (p' - q)_i \frac{1}{2\omega_{K^*}} \frac{1}{2\omega_K} \frac{1}{2\omega_D} \\
&\times \frac{1}{P^0 - \omega_D(\vec{p}' + \vec{q}) - \omega_{K^*}(\vec{p}' + \vec{q}) + i\varepsilon} \left( \frac{1}{P^0 - p'^0 - \omega_D(\vec{p}' + \vec{q}) - \omega_K(\vec{q}) + i\varepsilon} \right. \\
&\left. + \frac{1}{p'^0 - \omega_{K^*}(\vec{p}' + \vec{q}) - \omega_K(\vec{q}) + i\varepsilon} \right). \quad (15)
\end{aligned}$$

Next, considering that

$$\int d^3 q F(\vec{q}, \vec{p}') q_\ell = p'_\ell \int d^3 q F(\vec{q}, \vec{p}') \frac{\vec{q} \cdot \vec{p}'}{|\vec{p}'|^2}, \quad (16)$$

we finally write Eq. (15) as

$$t_{\text{loop}}^{(a)} = \mathcal{I}_{\text{loop}}^{(a)} (\vec{\varepsilon}_A \cdot \vec{p}'), \quad (17)$$

with  $\mathcal{I}_{loop}^{(a)}$  given by

$$\begin{aligned} \mathcal{I}_{loop}^{(a)} &= g g_{D_{s1}(2536), K^{*+} D^0} V_{D^0 K^0 \rightarrow D_s^+ \pi^-} \int \frac{d^3 q}{(2\pi)^3} \Theta(q_{\max} - |\vec{q} + \vec{p}'|) \Theta(\Lambda - |q^*|) \left(1 - \frac{\vec{q} \cdot \vec{p}'}{|\vec{p}'|^2}\right) \\ &\times \frac{1}{2\omega_{K^*}(\vec{p}' + \vec{q})} \frac{1}{2\omega_D(\vec{p}' + \vec{q})} \frac{1}{2\omega_K(\vec{q})} \frac{1}{P^0 - \omega_D(\vec{p}' + \vec{q}) - \omega_{K^*}(\vec{p}' + \vec{q}) + i\frac{\Gamma_{K^*}}{2}} \\ &\times \left( \frac{1}{P^0 - p'^0 - \omega_D(\vec{p}' + \vec{q}) - \omega_K(\vec{q}) + i\varepsilon} + \frac{1}{p'^0 - \omega_{K^*}(\vec{p}' + \vec{q}) - \omega_K(\vec{q}) + i\frac{\Gamma_{K^*}}{2}} \right), \end{aligned} \quad (18)$$

where  $\vec{p}'$  in this case, corresponds to the  $\pi^+$  momentum, namely,

$$\vec{p}' = \frac{\lambda^{\frac{1}{2}}(m_{D_{s1}}^2, m_{\pi^+}^2, M_{\text{inv}}^2(D_s^+ \pi^-))}{2m_{D_{s1}}}. \quad (19)$$

In Eq. (18) we have implemented two changes, the introduction of two  $\Theta$  functions and the explicit consideration of the  $K^*$  width. The appearance in Eq. (18) of a Heaviside theta function  $\Theta$  which sets the upper limit in the integral, comes naturally from the chiral unitary approach, which considers a separable potential of the form  $V(\vec{q}', \vec{q}) = V\Theta(q_{\max} - |\vec{q}'|) \Theta(q_{\max} - |\vec{q}|)$ , leading to  $T(\vec{q}', \vec{q}) = T\Theta(q_{\max} - |\vec{q}'|) \Theta(q_{\max} - |\vec{q}|)$ , where  $q_{\max}$  stands for the cutoff used to regularize the loops encoded in the  $G$ -function. In Ref. [51], the  $D_{s1}(2536)$  state is dynamically generated from  $DK^*$  interaction with  $q_{\max} = 1025$  MeV, which is the value we are considering in Eq. (18). Another theta function  $\Theta(\Lambda - |q^*|)$  is for the vertex  $D^0 K^0 \rightarrow D_s^+ \pi^-$ , where  $q^*$  is the three momentum of  $K^0$  boosted to  $D_s^+ \pi^-$  rest frame

$$q^* = \left[ \left( \frac{E_{D_s^+ \pi^-}}{M_{\text{inv}}(D_s^+ \pi^-)} - 1 \right) \frac{\vec{q} \cdot \vec{p}'}{|\vec{p}'|^2} + \frac{E_{K^0}}{M_{\text{inv}}(D_s^+ \pi^-)} \right] \cdot \vec{p}' + \vec{q}, \quad (20)$$

where  $E_{D_s^+ \pi^-} = \sqrt{M_{\text{inv}}^2(D_s^+ \pi^-) + |\vec{p}'|^2}$ ,  $E_{K^0} = \sqrt{m_{K^0}^2 + |\vec{q}|^2}$ . We calculate with  $\Lambda \equiv 600$  MeV and vary it within the range  $\Lambda \in [500, 700]$  MeV to estimate the uncertainty in our result as done in Ref. [47] (the change induced by changing  $q_{\max}$  are very small compared to those changing  $\Lambda$ ).

The triangle loop in Fig. 1(b) is readily obtained from Eq. (17) by setting  $\vec{p}' \rightarrow \vec{p}'_{\pi^-}$ , that is,

$$t_{\text{loop}}^{(b)} = \mathcal{I}_{\text{loop}}^{(b)}(\vec{\varepsilon}_A \cdot \vec{p}'_{\pi^-}), \quad (21)$$

where  $t_{\text{loop}}^{(b)}$  is

$$\mathcal{I}_{\text{loop}}^{(b)} = g g_{D_{s1}(2536), K^{*0} D^+} V_{D^+ K^+ \rightarrow D_s^+ \pi^+} \int \frac{d^3 q}{(2\pi)^3} \Theta(q_{\max} - |\vec{q} + \vec{p}'_{\pi^-}|) \Theta(\Lambda - |q^*|) \left(1 - \frac{\vec{q} \cdot \vec{p}'_{\pi^-}}{|\vec{p}'_{\pi^-}|^2}\right)$$

$$\begin{aligned}
& \times \frac{1}{2\omega_{K^*}(\vec{p}'_{\pi^-} + \vec{q})} \frac{1}{2\omega_D(\vec{p}'_{\pi^-} + \vec{q})} \frac{1}{2\omega_K(\vec{q})} \frac{1}{P^0 - \omega_D(\vec{p}'_{\pi^-} + \vec{q}) - \omega_{K^*}(\vec{p}'_{\pi^-} + \vec{q}) + i\frac{\Gamma_{K^*}}{2}} \\
& \times \left( \frac{1}{P^0 - p_{\pi^-}^0 - \omega_D(\vec{p}'_{\pi^-} + \vec{q}) - \omega_K(\vec{q}) + i\varepsilon} + \frac{1}{p_{\pi^-}^0 - \omega_{K^*}(\vec{p}'_{\pi^-} + \vec{q}) - \omega_K(\vec{q}) + i\frac{\Gamma_{K^*}}{2}} \right).
\end{aligned} \tag{22}$$

As a result, the total amplitude will be

$$t_{\text{total}} = \mathcal{I}_{\text{loop}}^{(a)} (\vec{\varepsilon}_A \cdot \vec{p}'_{\pi^+}) + \mathcal{I}_{\text{loop}}^{(b)} (\vec{\varepsilon}_A \cdot \vec{p}'_{\pi^-}), \tag{23}$$

where  $\vec{p}'_{\pi^+}$  and  $\vec{p}'_{\pi^-}$  are the  $\pi^+$  and  $\pi^-$  momenta in the  $D_{s1}$  rest frame,

$$\begin{aligned}
\vec{p}'_{\pi^+} &= \frac{\lambda^{\frac{1}{2}}(m_{D_{s1}}^2, m_{\pi^+}^2, m_{23}^2)}{2m_{D_{s1}}}, \\
\vec{p}'_{\pi^-} &= \frac{\lambda^{\frac{1}{2}}(m_{D_{s1}}^2, m_{\pi^-}^2, m_{13}^2)}{2m_{D_{s1}}},
\end{aligned} \tag{24}$$

with  $m_{23}$  and  $m_{13}$  standing for the invariant masses associated with the  $D_s^+\pi^-$  and  $D_s^+\pi^+$  pairs, respectively ( $\pi^+(1)$ ,  $\pi^-(2)$ ,  $D_s(3)$ ). Furthermore, these masses are not all independent, and by using

$$m_{12}^2 + m_{23}^2 + m_{13}^2 = m_{D_{s1}}^2 + m_{D_s^+}^2 + m_{\pi^+}^2 + m_{\pi^-}^2, \tag{25}$$

we can evaluate Eq. (23) as a function of the invariant masses that we are interested in.

Averaging over the  $D_{s1}$  polarizations, and taking the modulus squared of the amplitude in Eq. (23), that is

$$\overline{\sum} \sum |t_{\text{total}}|^2 = \frac{1}{3} \left\{ |\mathcal{I}_{\text{loop}}^{(a)}|^2 |\vec{p}'_{\pi^+}|^2 + |\mathcal{I}_{\text{loop}}^{(b)}|^2 |\vec{p}'_{\pi^-}|^2 + 2 \text{Re} [\mathcal{I}_{\text{loop}}^{(a)} \cdot (\mathcal{I}_{\text{loop}}^{(b)})^*] (\vec{p}'_{\pi^+} \cdot \vec{p}'_{\pi^-}) \right\}, \tag{26}$$

we are able to obtain the double differential invariant mass distribution [58], which is

$$\frac{d\Gamma}{dm_{12} dm_{23}} = \frac{1}{(2\pi)^3} \frac{2m_{12} 2m_{23}}{32m_{D_{s1}}^3} \overline{\sum} \sum |t_{\text{total}}|^2. \tag{27}$$

Since all the momenta involved and the scalar products in Eq. (26) are given in terms of the invariant masses  $m_{12}$ ,  $m_{23}$ , and  $m_{13}$ , by using Eq. (25) we can obtain the two-particle mass distribution in terms of any one of those invariant masses. For instance, for the  $m_{12}$  (the  $\pi^+\pi^-$ ) distribution we integrate Eq. (27) over  $m_{23}$ , such that

$$\frac{d\Gamma}{dm_{12}} = \int_{m_{23}^{\min}}^{m_{23}^{\max}} \frac{d\Gamma}{dm_{12} dm_{23}} dm_{23}, \tag{28}$$

with  $m_{23}^{\min}$ , and  $m_{23}^{\max}$  given by

$$\begin{aligned} m_{23}^{\min} &= \sqrt{(E_2 + E_3)^2 - (\sqrt{E_2^2 - m_2^2} + \sqrt{E_3^2 - m_3^2})^2}, \\ m_{23}^{\max} &= \sqrt{(E_2 + E_3)^2 - (\sqrt{E_2^2 - m_2^2} - \sqrt{E_3^2 - m_3^2})^2}. \end{aligned} \quad (29)$$

Moreover,  $E_2$ ,  $E_3$  are given by

$$\begin{aligned} E_2 &= \frac{m_{12}^2 - m_1^2 + m_2^2}{2m_{12}}, \\ E_3 &= \frac{m_{D_{s1}}^2 - m_{12}^2 - m_3^2}{2m_{12}}. \end{aligned} \quad (30)$$

All the other two-particle mass distribution are easily derived by taking cyclical permutations of the 1, 2, 3 indices in the expressions above.

### III. NUMERICAL RESULTS

The numerical results are presented in Figs. 2 and 3. Specifically, Fig. 2 illustrates the  $\pi^+\pi^-$  mass distribution. We can observe a smooth lineshape throughout the invariant mass range allowed by kinematics, including a broad peak in the range of 300 MeV to 400 MeV. It is interesting to mention that even if we do not have a direct  $\pi^+\pi^-$  interaction here, the shape of the mass distribution is quite different from one of pure phase space. This is due to the particular mechanism of  $D_s^+\pi^+\pi^-$  production, tied to the molecular nature of the  $D_{s1}(2536)$  and the triangle mechanism that follows as a consequence.

In Fig. 3, on the other hand, we notice a smooth curve throughout most of the distribution, except at the extremes, where two cusp structures are clearly visible: one around 2140 MeV and another, more pronounced, in the high-energy region of the spectrum, at approximately 2363 MeV. This latter value is associated with a threshold singularity, arising from the contribution of the  $D^0K^0 \rightarrow D_s^+\pi^-$  transition exactly at the  $D^0K^0$  production threshold, located at 2363 MeV. This threshold condition consequently generates a cusp at this energy.

Similarly, the small enhancement observed around 2140 MeV can be understood as a result of the on-shell contribution of the  $D^+K^+$  pair in the  $D^+K^+ \rightarrow D_s^+\pi^+$  transition. In particular, we expect the appearance of a cusp in the mass spectrum shown in Fig. 3, precisely at 2143 MeV, when the invariant mass of the  $D_s^+\pi^+$  system,  $m_{D_s^+\pi^+}$ , reaches approximately 2363 MeV.

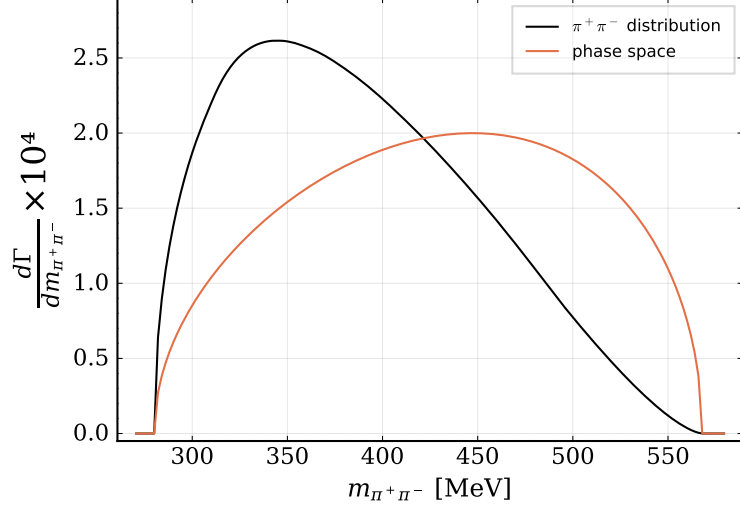


FIG. 2.  $\pi^+\pi^-$  invariant mass spectrum and phase space.

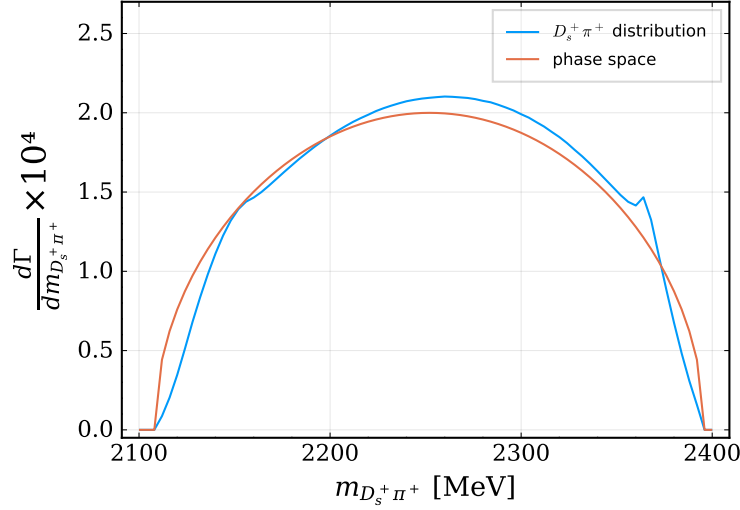


FIG. 3.  $D_s^+\pi^+$  invariant mass spectrum and phase space.

This correlation between the two values can be understood by noting that, in the rest frame of the  $D_s^+\pi^+$  pair, the invariant mass  $m_{D_s^+\pi^-}$  can be written as a function of  $m_{D_s^+\pi^+}$  through the relation

$$m_{D_s^+\pi^-}^2 = m_{\pi^-}^2 + m_{D_s^+}^2 + 2 E_{\pi^-} E_{D_s^+} - 2 (\vec{p}_{\pi^-} \cdot \vec{p}_{D_s^+}), \quad (31)$$

where  $\vec{p}_{\pi^-}$  and  $\vec{p}_{D_s^+}$  are the three-momenta of the  $\pi^-$  and  $D_s^+$  mesons, respectively, evaluated in the  $D_s^+\pi^+$  rest frame

$$\vec{p}_{\pi^-} = \frac{\lambda^{\frac{1}{2}}(m_{D_s^+}^2, m_{\pi^-}^2, M_{\text{inv}}^2(D_s^+\pi^+))}{2 M_{\text{inv}}(D_s^+\pi^+)},$$

$$\vec{p}_{D_s^+} = \frac{\lambda^{\frac{1}{2}} \left( M_{\text{inv}}^2(D_s^+\pi^+), m_{\pi^-}^2, m_{D_s^+}^2 \right)}{2 M_{\text{inv}}(D_s^+\pi^+)}. \quad (32)$$

Both  $E_{\pi^-}$ ,  $E_{D_s^+}$ , and the magnitudes of the momenta depend on  $m_{D_s^+\pi^+}$ . Therefore, by setting  $m_{D_s^+\pi^+} = 2363$  MeV, the above equation yields  $m_{D_s^+\pi^-} \approx 2143$  MeV, precisely where the corresponding cusp is expected to appear. It should be noticed that in this case the phase space distribution is similar to the actual one, except for the two cusps discussed above.

We do not plot the  $D_s^+\pi^-$  mass distribution which is very similar to the  $D_s^+\pi^+$  one (slight difference because of different masses of the intermediate states).

Given that our model has no free parameters, the invariant mass distribution curves are absolute, allowing us to compute the decay width of the  $D_{s1}(2536)$  meson. This width is obtained by determining the area under the spectral curves in Figs. 2 and 3, which should, of course, yield the same value. Consequently, we obtain the following value for the decay width of the  $D_{s1}(2536) \rightarrow D_s^+\pi^+\pi^-$  process

$$\Gamma(D_{s1}(2536) \rightarrow D_s^+\pi^+\pi^-) = 44 \pm 15 \text{ keV}, \quad (33)$$

where the uncertainty arises from the variation of the cutoff parameter  $\Lambda$ . This value is about an order of magnitude bigger than the one obtained in the  $D_{s1}(2460) \rightarrow D_s^+\pi^+\pi^-$  decay [47], which should make its observation feasible.

#### IV. SUMMARY

In summary, our study highlights the relevance of triangle loop mechanisms in the  $D_{s1}(2536) \rightarrow D_s^+\pi^+\pi^-$  decay process, where intermediate meson-meson interactions play a crucial role in shaping the final-state mass distributions. Within our model, we assume that the decay proceeds via such loops, adopting a molecular picture for the axial meson  $D_{s1}(2536)$ , where this state is dynamically generated through the  $DK^*$  interaction.

We have also emphasized the impact of dynamical effects driven by the proximity of intermediate thresholds. In the present study, these effects are particularly significant, giving rise to non-trivial structures in the spectra. Specifically, in the invariant mass distribution of the  $D_s^+\pi^+$  pair, the manifestation of threshold singularities becomes evident at values that coincide with the on-shell conditions of the intermediate  $D^0K^0$  and  $D^+K^+$  states.

Moreover, we have provided a parameter-free prediction for the  $D_{s1}(2536) \rightarrow D_s^+ \pi^+ \pi^-$  decay width, ensuring that the evaluated mass spectra represents absolute values for the process under consideration.

Overall, these findings offer further insight into the role of hadronic loops and final-state interactions in shaping observable features—such as cusps and enhancements—in multi-body decay processes of heavy mesons.

## ACKNOWLEDGMENTS

This work is supported by the Spanish Ministerio de Economía y Competitividad (MINECO) and European FEDER funds under Contracts No. FIS2017-84038-C2-1-P-B, PID2020-112777GB-I00, and by Generalitat Valenciana under contract PROMETEO/2020/023. This project has received funding from the European Union Horizon 2020 research and innovation programme under the program H2020-INFRAIA-2018-1, grant agreement No. 824093 of the STRONG-2020 project. This work is supported by the Spanish Ministerio de Ciencia e Innovación (MICINN) under contracts PID2020-112777GB-I00, PID2023-147458NB-C21 and CEX2023-001292-S; by Generalitat Valenciana under contracts PROMETEO/2020/023 and CIPROM/2023/59. Yi-Yao Li is supported in part by the Guangdong Provincial international exchange program for outstanding young talents of scientific research in 2024.

- 
- [1] H.-X. Chen, W. Chen, X. Liu, and S.-L. Zhu, *Phys. Rept.* **639**, 1 (2016), [arXiv:1601.02092 \[hep-ph\]](#).
  - [2] R. F. Lebed, R. E. Mitchell, and E. S. Swanson, *Prog. Part. Nucl. Phys.* **93**, 143 (2017), [arXiv:1610.04528 \[hep-ph\]](#).
  - [3] A. Esposito, A. Pilloni, and A. D. Polosa, *Phys. Rept.* **668**, 1 (2017), [arXiv:1611.07920 \[hep-ph\]](#).
  - [4] N. Brambilla, S. Eidelman, C. Hanhart, A. Nefediev, C.-P. Shen, C. E. Thomas, A. Vairo, and C.-Z. Yuan, *Phys. Rept.* **873**, 1 (2020), [arXiv:1907.07583 \[hep-ex\]](#).

- [5] F.-K. Guo, C. Hanhart, U.-G. Meißner, Q. Wang, Q. Zhao, and B.-S. Zou, *Rev. Mod. Phys.* **90**, 015004 (2018), [Erratum: *Rev.Mod.Phys.* 94, 029901 (2022)], [arXiv:1705.00141 \[hep-ph\]](#).
- [6] R. M. Albuquerque, J. M. Dias, K. P. Khemchandani, A. Martínez Torres, F. S. Navarra, M. Nielsen, and C. M. Zanetti, *J. Phys. G* **46**, 093002 (2019), [arXiv:1812.08207 \[hep-ph\]](#).
- [7] H. Albrecht *et al.* (ARGUS), *Phys. Lett. B* **230**, 162 (1989).
- [8] J. P. Alexander *et al.* (CLEO), *Phys. Lett. B* **303**, 377 (1993).
- [9] B. Aubert *et al.* (BaBar), *Phys. Rev. D* **77**, 011102 (2008), [arXiv:0708.1565 \[hep-ex\]](#).
- [10] J. P. Lees *et al.* (BaBar), *Phys. Rev. D* **83**, 072003 (2011), [arXiv:1103.2675 \[hep-ex\]](#).
- [11] S. Jia *et al.* (Belle), *Phys. Rev. D* **100**, 111103 (2019), [arXiv:1911.00671 \[hep-ex\]](#).
- [12] R. Aaij *et al.* (LHCb), *JHEP* **10**, 106, [arXiv:2308.00587 \[hep-ex\]](#).
- [13] A. Dougall, R. D. Kenway, C. M. Maynard, and C. McNeile (UKQCD), *Phys. Lett. B* **569**, 41 (2003), [arXiv:hep-lat/0307001](#).
- [14] Y.-B. Dai, C.-S. Huang, C. Liu, and S.-L. Zhu, *Phys. Rev. D* **68**, 114011 (2003), [arXiv:hep-ph/0306274](#).
- [15] D. Ebert, V. O. Galkin, and R. N. Faustov, *Phys. Rev. D* **57**, 5663 (1998), [Erratum: *Phys.Rev.D* 59, 019902 (1999)], [arXiv:hep-ph/9712318](#).
- [16] S. Godfrey and N. Isgur, *Phys. Rev. D* **32**, 189 (1985).
- [17] Y. S. Kalashnikova, A. V. Nefediev, and Y. A. Simonov, *Phys. Rev. D* **64**, 014037 (2001), [arXiv:hep-ph/0103274](#).
- [18] V. Balagura *et al.* (Belle), *Phys. Rev. D* **77**, 032001 (2008), [arXiv:0709.4184 \[hep-ex\]](#).
- [19] M. Bishai *et al.* (CLEO), *Phys. Rev. D* **57**, 3847 (1998), [arXiv:hep-ex/9710023](#).
- [20] R. N. Cahn and J. D. Jackson, *Phys. Rev. D* **68**, 037502 (2003), [arXiv:hep-ph/0305012](#).
- [21] D. Ebert, R. N. Faustov, and V. O. Galkin, *Eur. Phys. J. C* **66**, 197 (2010), [arXiv:0910.5612 \[hep-ph\]](#).
- [22] E. E. Kolomeitsev and M. F. M. Lutz, *Phys. Lett. B* **582**, 39 (2004), [arXiv:hep-ph/0307133](#).
- [23] D. Gamermann and E. Oset, *Eur. Phys. J. A* **33**, 119 (2007), [arXiv:0704.2314 \[hep-ph\]](#).
- [24] F.-K. Guo, P.-N. Shen, H.-C. Chiang, R.-G. Ping, and B.-S. Zou, *Phys. Lett. B* **641**, 278 (2006), [arXiv:hep-ph/0603072](#).
- [25] F.-K. Guo, P.-N. Shen, and H.-C. Chiang, *Phys. Lett. B* **647**, 133 (2007), [arXiv:hep-ph/0610008](#).
- [26] S.-Y. Kong, J.-T. Zhu, D. Song, and J. He, *Phys. Rev. D* **104**, 094012 (2021), [arXiv:2106.07272](#)

- [hep-ph].
- [27] F. Aceti, M. Bayar, E. Oset, A. Martinez Torres, K. P. Khemchandani, J. M. Dias, F. S. Navarra, and M. Nielsen, *Phys. Rev. D* **90**, 016003 (2014), arXiv:1401.8216 [hep-ph].
- [28] J. M. Dias, F. Aceti, and E. Oset, *Phys. Rev. D* **91**, 076001 (2015), arXiv:1410.1785 [hep-ph].
- [29] F. Aceti, M. Bayar, J. M. Dias, and E. Oset, *Eur. Phys. J. A* **50**, 103 (2014), arXiv:1401.2076 [hep-ph].
- [30] J. A. Oller and E. Oset, *Nucl. Phys. A* **620**, 438 (1997), [Erratum: *Nucl.Phys.A* 652, 407–409 (1999)], arXiv:hep-ph/9702314.
- [31] L. Roca, E. Oset, and J. Singh, *Phys. Rev. D* **72**, 014002 (2005), arXiv:hep-ph/0503273.
- [32] N. Kaiser, P. B. Siegel, and W. Weise, *Nucl. Phys. A* **594**, 325 (1995), arXiv:nucl-th/9505043.
- [33] E. Oset and A. Ramos, *Nucl. Phys. A* **635**, 99 (1998), arXiv:nucl-th/9711022.
- [34] J. A. Oller and U. G. Meissner, *Phys. Lett. B* **500**, 263 (2001), arXiv:hep-ph/0011146.
- [35] D. Jido, J. A. Oller, E. Oset, A. Ramos, and U. G. Meissner, *Nucl. Phys. A* **725**, 181 (2003), arXiv:nucl-th/0303062.
- [36] T. Hyodo, D. Jido, and A. Hosaka, *Phys. Rev. C* **78**, 025203 (2008), arXiv:0803.2550 [nucl-th].
- [37] T. Hyodo, D. Jido, and A. Hosaka, *Phys. Rev. C* **85**, 015201 (2012), arXiv:1108.5524 [nucl-th].
- [38] T. Sekihara, T. Hyodo, and D. Jido, *PTEP* **2015**, 063D04 (2015), arXiv:1411.2308 [hep-ph].
- [39] X.-K. Dong, F.-K. Guo, and B.-S. Zou, *Commun. Theor. Phys.* **73**, 125201 (2021), arXiv:2108.02673 [hep-ph].
- [40] X.-K. Dong, F.-K. Guo, and B. S. Zou, *Few Body Syst.* **62**, 61 (2021).
- [41] X.-K. Dong, F.-K. Guo, and B.-S. Zou, *Progr. Phys.* **41**, 65 (2021), arXiv:2101.01021 [hep-ph].
- [42] F.-K. Guo, C. Hidalgo-Duque, J. Nieves, and M. P. Valderrama, *Phys. Rev. D* **88**, 054007 (2013), arXiv:1303.6608 [hep-ph].
- [43] C. Garcia-Recio, M. F. M. Lutz, and J. Nieves, *Phys. Lett. B* **582**, 49 (2004), arXiv:nucl-th/0305100.
- [44] G.-J. Wang, L.-Y. Xiao, R. Chen, X.-H. Liu, X. Liu, and S.-L. Zhu, *Phys. Rev. D* **102**, 036012 (2020), arXiv:1911.09613 [hep-ph].
- [45] E. Oset *et al.*, *Int. J. Mod. Phys. E* **25**, 1630001 (2016), arXiv:1601.03972 [hep-ph].
- [46] M.-N. Tang, Y.-H. Lin, F.-K. Guo, C. Hanhart, and U.-G. Meißner, *Commun. Theor. Phys.* **75**, 055203 (2023), arXiv:2303.18225 [hep-ph].
- [47] L. Roca, J. M. Dias, and E. Oset, *Eur. Phys. J. C* **85**, 808 (2025), arXiv:2502.18401 [hep-ph].

- [48] N. Kaiser, [Eur. Phys. J. A \*\*3\*\*, 307 \(1998\)](#).
- [49] J. Nieves and E. Ruiz Arriola, [Phys. Lett. B \*\*455\*\*, 30 \(1999\)](#), [arXiv:nucl-th/9807035](#).
- [50] R. Aaij *et al.* (LHCb), Study of  $D_{s1}(2460)^+ \rightarrow D_s^+ \pi^+ \pi^-$  in  $B \rightarrow \bar{D}^{(*)} D_s^+ \pi^+ \pi^-$  decays (2024), [arXiv:2411.03399 \[hep-ex\]](#).
- [51] J.-X. Lin, H.-X. Chen, W.-H. Liang, C.-W. Xiao, and E. Oset, [Eur. Phys. J. C \*\*84\*\*, 439 \(2024\)](#), [arXiv:2401.04587 \[hep-ph\]](#).
- [52] M. Bando, T. Kugo, S. Uehara, K. Yamawaki, and T. Yanagida, [Phys. Rev. Lett. \*\*54\*\*, 1215 \(1985\)](#).
- [53] M. Bando, T. Kugo, and K. Yamawaki, [Phys. Rept. \*\*164\*\*, 217 \(1988\)](#).
- [54] U. G. Meissner, [Phys. Rept. \*\*161\*\*, 213 \(1988\)](#).
- [55] H. Nagahiro, L. Roca, A. Hosaka, and E. Oset, [Phys. Rev. D \*\*79\*\*, 014015 \(2009\)](#), [arXiv:0809.0943 \[hep-ph\]](#).
- [56] A. Bramon, A. Grau, and G. Pancheri, [Phys. Lett. B \*\*283\*\*, 416 \(1992\)](#).
- [57] S. Sakai, E. Oset, and A. Ramos, [Eur. Phys. J. A \*\*54\*\*, 10 \(2018\)](#), [arXiv:1705.03694 \[hep-ph\]](#).
- [58] S. Navas *et al.* (Particle Data Group), [Phys. Rev. D \*\*110\*\*, 030001 \(2024\)](#).